Supporting Information

Integrated energy storage and electrochromic function in one flexible device: an energy storage smart window

Kai Wang[a, b], *Haiping Wu*[a, b], *Yuena Meng*[a, b], *Yajie Zhang*[a], *and Zhixiang Wei* [*, a]

[†]National Center for Nanoscience and Technology, Beijing 100190, P. R. China, and
[‡]Graduate School of the Chinese Academy of Sciences, Beijing 100190, P. R. China

Email: weizx@nanoctr.cn

1. Preparation of gel electrolyte

Firstly, 1 g polyvinyl alcohol (PVA) powder (medium molecular weight, Alfa Aesar) was added into 10 ml deionized water with vigorous stirring and subsequent heating under stirring to ~85°C until the solution becomes clear. Then, PVA gel was coated to the surface of electrode by using a scribing knife. After solidified, a certain amount of 1M H_2SO_4 aqueous solution was dipped to PVA film and coated by using a scribing knife prior to assembly of the ESS window. The weight ratio between H_2SO_4 and PVA is about 1:1.

2 The effect of PEDOT: PSS layer

Commercial available PEDOT: PSS film showed excellent conductivity under a wide potential window (-1V – 1V) in an electrochemical system. Besides, it possessed a neglectable capacitance compared with active materials PANI (not shown here). Furthermore, the electrode exhibited a good light transmission (c.a. 95%) after coating PEDOT: PSS on the PET substrate. Thus, PEDOT: PSS was employed as current collector for active materials (Figure S1a). According to our results, the PEDOT: PSS layer played an important role in reducing the inner resistance of device. CVs

were used to explain the effect of PEDOT: PSS layer to device performance. When a low scan rate was employed to device, the shape of CV curves was similar as shown in Figure S1b. However, when the scan rates were improved, the shape of CV curves of different devices would deviate. The CV curves of PANI electrode would incline if no conductive layer (Figure S1c, d). That was because the conductivity of active PANI material was bad when it was under leucoemeraldine and pernigraniline state. So the large IR drop of active material resulted in the incline of CV curves.

3 The areal capacitance calculation

The areal capacitance (F cm $^{-2}$) was measured by both CV curves and galvanostatic charge-discharge methods.

From CV curves, the areal capacitances in different scanning rates were calculated according to the following equation:

$C=2(\int IdV)/(V\nu S)$

Where I denote as the current in the CV curve, V represents the potential window, ν is the potential scanning rate, and S is the active materials surface area of the single electrodes (cm^2).

Areal capacitance of supercapacitors is calculated according to the following equation when using the galvanostatic charge-discharge curves (as shown in Figure S2):

$C = 2\times I\times t / (V\times S)$

Where C is areal capacitance (F cm^{-2}), I stands for discharge current (mA), t is the discharge time (s), V represents the potential window (V), and S is the active materials surface area of the single electrodes (cm^2).

4 Galvanostatic charge - discharge curves and IR drop

Figure S3 was Galvanostatic charge – discharge curves and IR drop at different current densities. The shape of Galvanostatic charge-discharge curves of ESS window shows a typical pseudo-capacitance characteristic. The voltage versus time curve of pseudocapacitors is different with electric double layer capacitor (EDLC). For EDLC, it is a triangular shape due to voltage change linearly as times increase. But pseudocapacitors show a non-ideal triangular shape due to redox process, which is a typical pseudocapacitance characteristic. Besides, IR drop in charge-discharge curves can also be investigated. Generally, IR drop is resulted from electrolyte potential drop and contact resistance, and it is also depend on charge-discharge current density. From discharge curves at different current densities, the IR drop is

obviously observed and increased from 15 mV at 0.01 mA cm $^{-2}$ to 400 mV at 0.3 mA cm $^{-2}$, respectively. The PANI electrode possesses better electric conductivity (72 S cm^{-1}) than polymer electrolyte used in our experiment, so the IR drop is proposed mainly ascribed from electrolyte potential drop.

5 The voltage decay and leakage current of the device

As a potential energy storage unit integrated with other devices, the self-discharge and leakage current of the device are necessary concerns. The device was first cycled between 0–0.7 V for two cycles before the self-discharge test. And then, the device was charged to 0.7V to note the open-circuit potential decay. Figure S4 a was voltage decay plot as the time increase that was used to evaluate the self-discharge phenomenon of device. From the plot, the potential can be kept in the 0.35V even after about 10 hours, which showed a low self-discharge property. Furthermore, the leakage current was noted when the device was charged to 0.7v after being first cycled between 0–0.7 V for two cycles, as seen as in Figure S4 b. From the results, our ESS window shows a low leakage current. The leakage current was about 17 μA at the beginning, and further decreased to 2 μA which was even ignored. The low self-discharge and leakage showed that our ESS window has a large potential application.

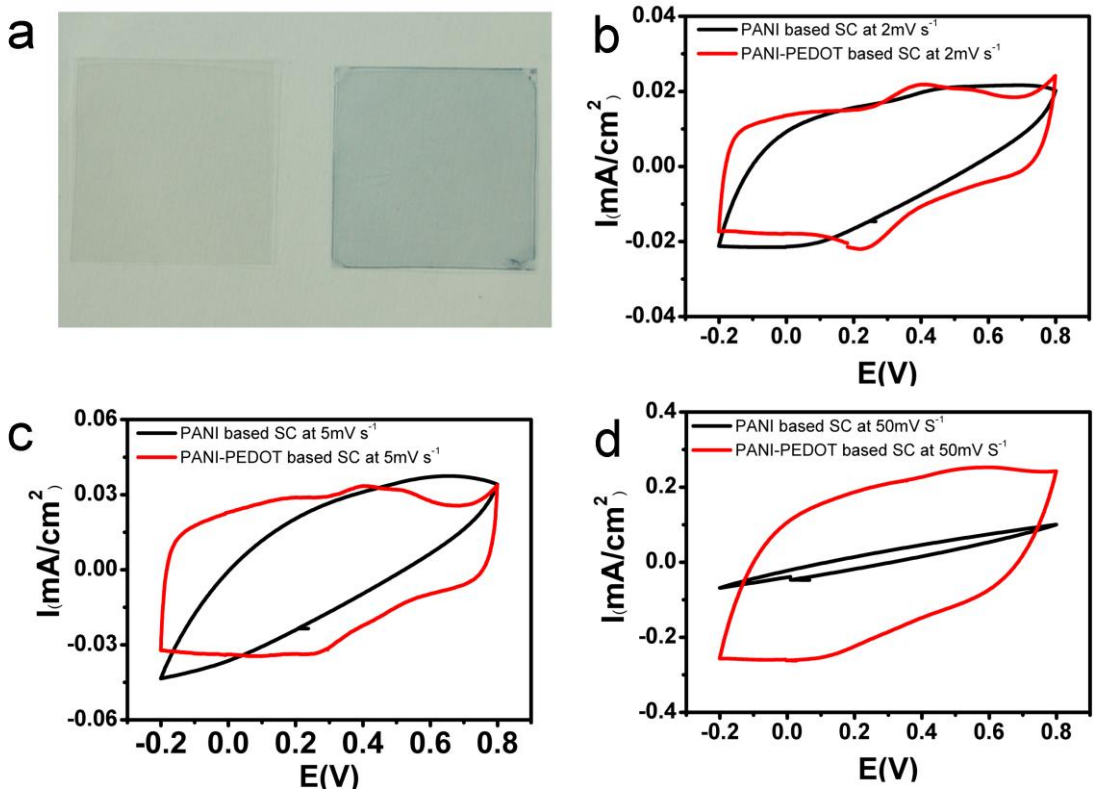

Figure S1 (a) Left is a transparent PET substrate, and the right is PEDOT: PSS coating –PET. (b, c, d) CV curves of intelligent supercapacitor with or without PEDOT: PSS coating and different scanning rates (2mV S^{-1}, 5mV S^{-1} and 50mV S^{-1}).

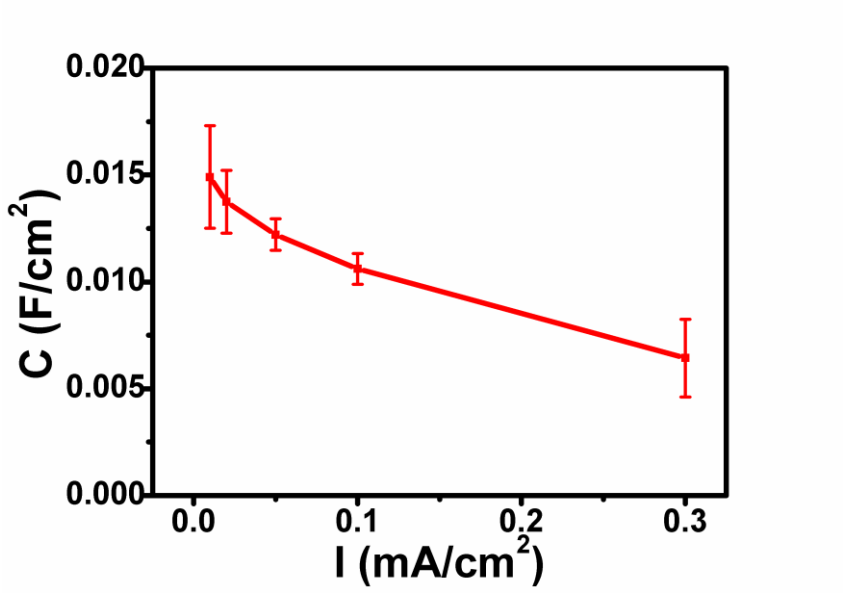

Figure S2 Areal capacitance plots as the current density increases calculated from Galvanostatic charge-discharge curves.

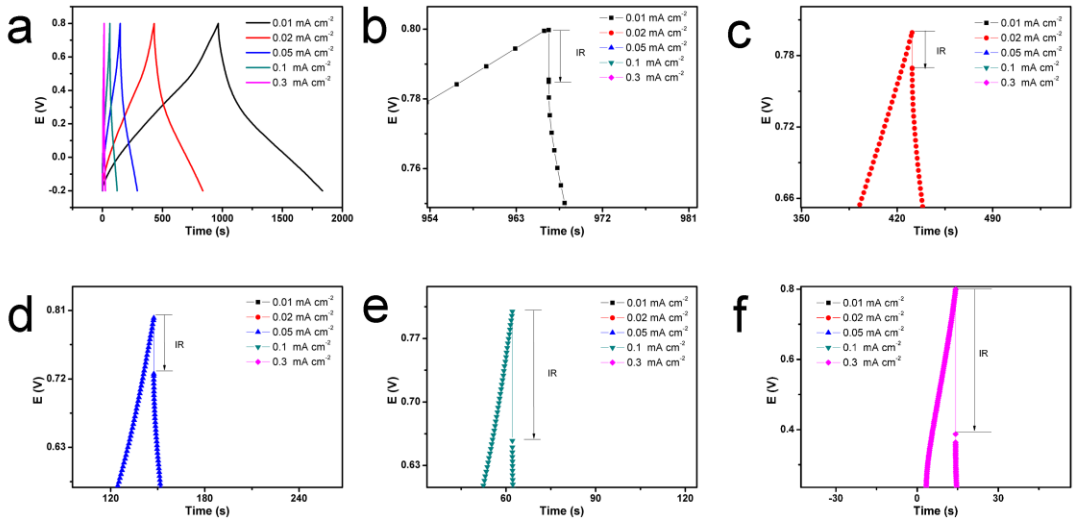

Figure S3 (a) Galvanostatic charge-discharge curves and IR drop in Galvanostatic charge-discharge curves at different current densities, (b) 0.01 mA cm^{-2}, (c) 0.02 mA cm^{-2} , (d) 0.05 mA cm^{-2}, (e) 0.1 mA cm^{-2}, (f) 0.3 mA cm^{-2}.

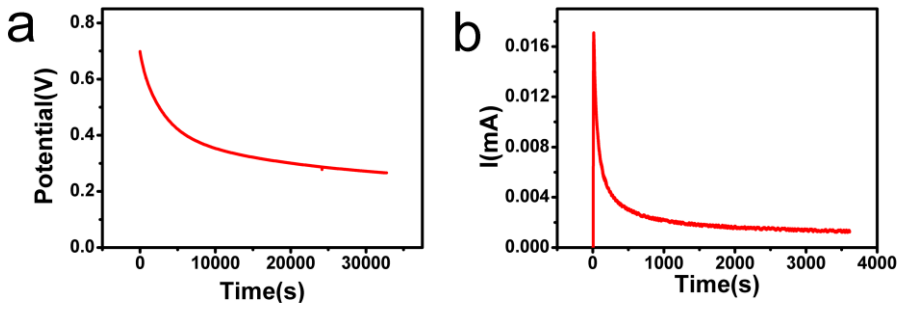

Figure S4 (a) Open potential curve versus time; (b) Leakage current versus time curves recorded with a chronoampermetry under a constant potential of 0.75 V.